Instantaneous mesh load factor (K_3) measurements in a wind turbine gearbox using fiber-optic strain sensors

Gutierrez-Santiago, Unai; Keller, Jonathan; Fernández-Sisón, Alfredo; Polinder, Henk; Van Wingerden, Jan Willem

DOI
10.1088/1742-6596/2767/4/042022

Publication date
2024

Document Version
Final published version

Published in
Journal of Physics: Conference Series

Instantaneous mesh load factor (K_γ) measurements in a wind turbine gearbox using fiber-optic strain sensors

Journal of Physics: Conference Series **2767** (2024) 042022 doi:10.1088/1742-6596/2767/4/042022

Instantaneous mesh load factor (K_γ) measurements in a wind turbine gearbox using fiber-optic strain sensors

Unai Gutierrez-Santiago[1,2], Jonathan Keller[3], Alfredo Fernández-Sisón[2], Henk Polinder[1], Jan-Willem van Wingerden[1]

[1] Technical University of Delft, Faculty of Mechanical Engineering, Mekelweg 2, 2628 CD, Delft, The Netherlands
[2] Siemens Gamesa Renewable Energy, Parque Tecnológico de Bizkaia, 48170 Zamudio, Spain
[3] National Renewable Energy Laboratory, 15013 Denver West Parkway Golden, CO 80401

E-mail: u.gutierrezsantiago@tudelft.nl

Abstract. The mesh load factor, K_γ, describes how loads are shared between planet gears and has become one of the key design challenges in modern wind turbine gearboxes. Planet load sharing directly impacts tooth root stresses, a critical driver of torque density and gearbox reliability. Experimental evaluation of K_γ is typically performed from sun gear tooth root strain gauge measurements, which are complex. Furthermore, such measurements can only provide an average value of load sharing. The present study describes an alternative method to evaluate the mesh load factor in wind turbine gearboxes based on fiber-optic strain sensors installed on the outer surface of the fixed ring gear. We present the results of an extensive measurement campaign to evaluate this novel sensing solution installed on the input planetary stage of a 2-MW wind turbine gearbox at the National Renewable Energy Laboratory's Flatirons Campus (Colorado, USA). The number of strain sensors on the ring gear was selected as an integer multiple of the number of planets, which has enabled an instantaneous evaluation of the mesh load factor. The effect of operating conditions on the planet load-sharing behavior of the gearbox has been investigated. The mesh load factor measured for operating conditions close to rated was below 1.05, well below IEC 61400-4 standard requirements.

1. Introduction

The push to lower the levelized cost of energy from wind has resulted in a race to increase the rotor diameter, power rating, and hub height of wind turbines [1]. The increased rated power and rotor diameters have significantly increased the rotor torque. This has translated into higher torque density demands for all drivetrain components and notably for the gearbox. Thanks to multiple technological innovations, torque densities of 200 $\mathrm{N\,m\,kg^{-1}}$ are now available [2, 3, 4]. For such high torque ratings, a trend has emerged in gearbox architecture to increase the number of planetary stages and the number of planets per stage [5]. The main challenge of such gearbox designs is sharing the load evenly between the planets, especially when subjected to rotor nontorque loads and in the presence of any manufacturing errors [6]. The gear rating standard ISO 6336-1 [7] defines the mesh load factor, K_γ, as the quotient between the highest load carried by a single planet divided by the average load of all planets. Within the design requirements for wind turbine gearboxes, the standard IEC 61400–4 [8] sets K_γ as a function

of the number of planets. For a large number of planets, the specified mesh load factors are conservative and would lead to gearbox designs with poor torque density. The standard allows using lower mesh load factors if they are experimentally demonstrated by gear tooth root strain gauge measurements. However, such measurements are very complex and costly and only provide an average measurement of the mesh load factor because the mesh intensity can only be assessed when an instrumented sun tooth meshes with the different planets. Because those gear meshes occur at different times, the mesh load factor has to be averaged over multiple revolutions of the sun gear relative to the carrier, assuming that the loading conditions remain constant during the averaging period. In [9], the authors presented an alternative approach based on strain measurements on the outer surface of the static ring gear. Because the ring gear is static, the system's complexity is greatly reduced and has the potential to be implemented on serial production gearboxes throughout their operational life instead of being limited to prototype verification purposes. Both methods yielded equivalent average mesh load factor results under stationary conditions. However, that study was performed on a back-to-back test bench under torque-only loading and stationary conditions. The number and placement of the strain sensors used did not allow the evaluation of simultaneous mesh events because they were not an integer multiple of the number of planets.

Planet load sharing directly impacts tooth root stresses, which are a critical driver of torque density and gearbox reliability. The ability to instantaneously measure the mesh load factor is important to verify design assumptions. Gear fatigue life calculations in gear rating standards assume a constant mesh load factor; measuring the mesh load factor instantaneously will verify the design assumptions for different operating conditions. The contribution of this paper is twofold: (1) We demonstrate that fiber-optic strain sensors with improved sensor placement can provide instantaneous measurements of the mesh load factor, and (2) we present the results of an extensive measurement campaign on a 2-MW wind turbine with nonstationary operating conditions and complex rotor loading.

The remainder of this paper is organized as follows: Section 2 describes the sensors and data acquisition equipment used for the experiment; Section 3 describes the methodology used to extract the instantaneous mesh load from fiber-optic strain measurements on the outer surface of the ring gear; Section 4 discusses the results obtained during the field measurement campaign; and finally, Section 5 draws the main conclusions of this work and suggests recommendations for future work.

2. Experimental set-up

The present study was conducted on a Gamesa G97 2-MW wind turbine, shown in Figure 1, located at the National Renewable Energy Laboratory's (NREL's) Flatirons Campus (Colorado, USA). This turbine has a four-point mount drivetrain, and the gearbox planetary stage comprises three planets. During the test campaign, data were collected from four different sources: (1) the fiber-optic strain sensors installed on the outer surface of the ring gear; (2) main shaft instrumentation comprising strain gauges and an angular encoder installed to measure torque, bending, and rotor azimuth angle; (3) NREL's meteorological tower to measure ambient temperature, wind speed, and wind direction at hub height; and (4) turbine controller for wind turbine operational parameters.

2.1. Fiber-optic sensors

An array of 24 fiber-optic strain sensors were installed around the outer surface of the ring gear of the gearbox, which has a single planetary stage. The sensing principle was based on Fiber Bragg Gratings (FBGs). FBGs are modifications to the fiber's core in discrete, short segments that reflect particular wavelengths of light and transmit all others. FBGs are suitable for sensing applications because the reflected wavelength is sensitive to temperature and strain changes

Figure 1. G97 2-MW wind turbine on NREL's Flatirons Campus. Photo from Dennis Schroeder, NREL 21886.

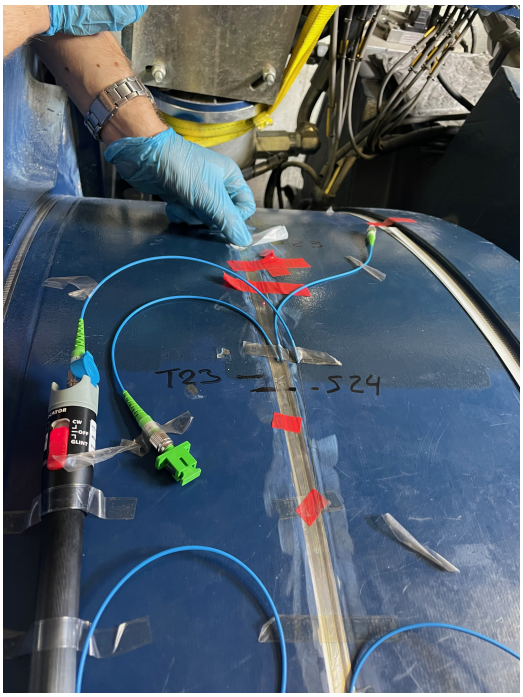

Figure 2. FBG installation. Photo from Unai Gutierrez-Santiago, Siemens Gamesa Renewable Energy, NREL 85910.

at the grating. FBGs offer a higher signal-to-noise ratio than traditional strain gauges based on their electrical resistance change. They are immune to electromagnetic interference, and a single optical fiber can accommodate multiple sensors, simplifying the installation process. In the present study, two optical fibers, each with 12 FBGs, were bonded with cyanoacrylate glue on the outer surface of the ring gear at the midpoint of the tooth width, as shown in Figure 2.

The 24 fiber-optic sensors were chosen as a multiple of the three planets. The sensors were equally spaced around the perimeter to ensure that the mesh events caused by the three planets could be detected simultaneously. Figure 3 shows a rotor side view of the middle section of the ring gear with the angular location of the strain sensors. In operation, the mesh forces between the planets and ring gear teeth cause deformations of the ring gear proportionate to the rotor torque. The main element of the data acquisition system is a fiber interrogator that sends light into the fiber and analyzes the wavelengths reflected by the gratings. The interrogator extracts a signal from each grating to measure strain and temperature. The interrogator used for the measurement campaign provided a sampling frequency of 2000 Hz for each signal. Sensing360 B.V. supplied the fiber optic sensors.

2.2. Main shaft sensors

The second set of sensors was installed in the main shaft. An angular displacement encoder measured absolute azimuth angle to relate the strains measured in the static ring gear to an angular position of the main shaft and rotor. A zero-degree azimuth angle was set with a blade labeled as "A" down. In the main shaft, three full Wheatstone bridges measured torque and the two orthogonal bending moments. All sensors installed in the main shaft were logged at a sampling rate of 60 Hz.

2.3. Meteorological data
The inflow wind conditions were gathered from the NREL Flatirons Campus M4/site 4.4 meteorological tower. Wind speed, wind direction, and temperature measurements at hub height were logged at a sampling rate of 60 Hz.

2.4. Turbine operation parameters
The last data source was the turbine controller. Using a proprietary data acquisition system supplied by Siemens Gamesa, several operational parameters were logged with a sampling frequency of 25 Hz. These operational parameters included the wind speed measured by the turbine, nacelle direction, total power produced, generator and rotor speed, gearbox oil sump and high-speed shaft bearing temperature, nacelle and exterior temperature, pitch angles, and pitch angle rates.

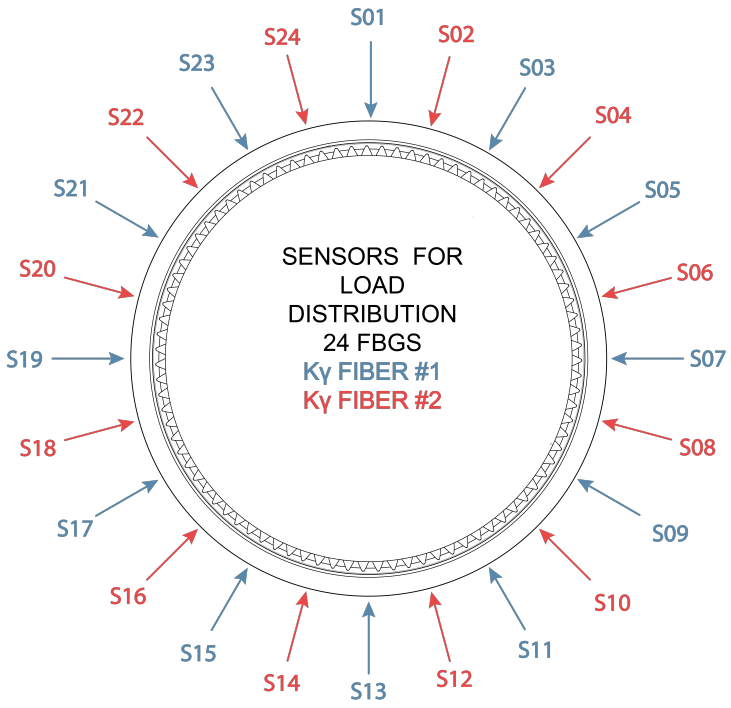

Figure 3. Angular placement of the 24 FBGs on the outer surface of the first-stage ring gear.

3. Evaluation of the load mesh factor from ring gear outer surface strain
The standard IEC 61400–4 [8] sets the design requirements for wind turbine gearboxes and specifies the mesh load factor K_γ as a function of the number of planets. The standard allows using lower mesh load factors if they are experimentally demonstrated by gear tooth root strain gauge measurements. Examples of practical implementations of such measurement systems can be found in [10] and [11]. Strain gauges must be placed in a root of the rotating sun gear to extract planet load-sharing behavior, which requires either a slip ring or telemetry system with appreciable planning and installation costs. Each time the instrumented sun tooth engages with a planet, the mesh forces can be evaluated, assuming they are proportional to a weighted sum of all the strains measured along the root. The instrumented tooth will mesh with all the planets because the sun rotates faster than the carrier. However, the mesh events do not

coincide in time. Therefore, the effect of the dynamic factor, K_{v}, and torque fluctuations must be addressed, and only an average value of the mesh load factor over multiple revolutions of the sun gear relative to the carrier can be obtained. A more elaborate way of evaluating the mesh load factor has been used to overcome this limitation [6]; however, this method is very complex and requires modifications to the gearbox and planet bearings. Using fiber-optic strain sensors, strain measurements on the ring gear's outer surface were proven to provide equivalent load-sharing results [9]. These results were obtained in a back-to-back test bench under stationary torque loads. Because the ring gear is stationary, there is no need for wireless data transfer, and the power supply is also simplified compared to when the instrumentation is on the rotating sun. However, with the sensor configuration used in [9], it was only possible to assess the average mesh load factor due to the chosen sensor spacing. For this study, a new sensor configuration, shown in Figure 3 and described in Section 2, was designed to evaluate the instantaneous planet load sharing.

For the G97 drivetrain, the rotor torque is transmitted directly by the main shaft to the planet carrier of the gearbox, which is then distributed by the carrier to the three planets. When the planets mesh with the ring gear, the mesh force causes the ring gear to deform, and this deformation is measured by the fiber-optic strain sensors placed on the ring gear's outer surface as a tensile-compressive cycle. FBGs are sensitive to changes in strain and temperature. However, temperature changes occur at a much lower pace than strain changes caused by gear mesh events. A moving average filter was used to detrend the raw FBG signals, and we assumed that once the long-term shift caused by temperature had been removed, the remaining signal was entirely caused by the strain imposed by the planet gear mesh events. The relationship between torque and the peak-to-peak values of the tensile-compressive strain cycle were described in [5]. Using the absolute rotor azimuth signal, the relative position of the planet carrier is known, and peak-to-peak values can be assigned to individual planets. Figure 4 shows the strain measured at sensor S01 and the azimuth angle. Arbitrarily, for each full rotation of the rotor, the first planet to cause a deformation in sensor S01 was identified as planet one (P1). During normal operation, the carrier rotates clockwise, downwind, and subsequent planets were labeled two (P2) and three (P3). For each sensor, the maxima and minima peaks of every revolution are detected and assigned to each planet, denoting the peak-to-peak strain as $\Delta\epsilon_{n,p}$, where n is the revolution number, and p is the planet number. For clarity, only the first revolution is shown in Figure 4. An average K_γ value can be computed for each sensor using the following equation, $\Delta\epsilon$

$$K_{\gamma,p} = \frac{\overline{\Delta\epsilon}_p}{\overline{\Delta\epsilon}_{all}}\,, \tag{1}$$

where $\overline{\Delta\epsilon}_p$ is the average peak-to-peak strain value measured from all mesh events assigned to a single planet, and $\overline{\Delta\epsilon}_{all}$ is the average peak-to-peak value of all planets. That is,

$$\overline{\Delta\epsilon}_p = \frac{1}{n}\sum_{i=1}^{n}\Delta\epsilon_{i,p} = \frac{\Delta\epsilon_{1,p} + \Delta\epsilon_{2,p} + \cdots + \Delta\epsilon_{n,p}}{n} \tag{2}$$

In the instrumentation setup used for this study, the number of strain sensors on the ring gear was selected as an integer multiple of the number of planets. Therefore, when a planet is meshing near a strain sensor, the other two planets are also close to other strain sensors, and it is possible to compare their strain peaks simultaneously. Since we have 24 sensors and three planets, there are eight possible sensor combinations with synchronous mesh events. Figure 5 shows one of the combinations with strain sensors S01, S09 and S17. The strains measured at each sensor location are different in magnitude. This was also observed when estimating the torque from the peak-to-peak values in [5]. A weighting or scaling of the individual peaks

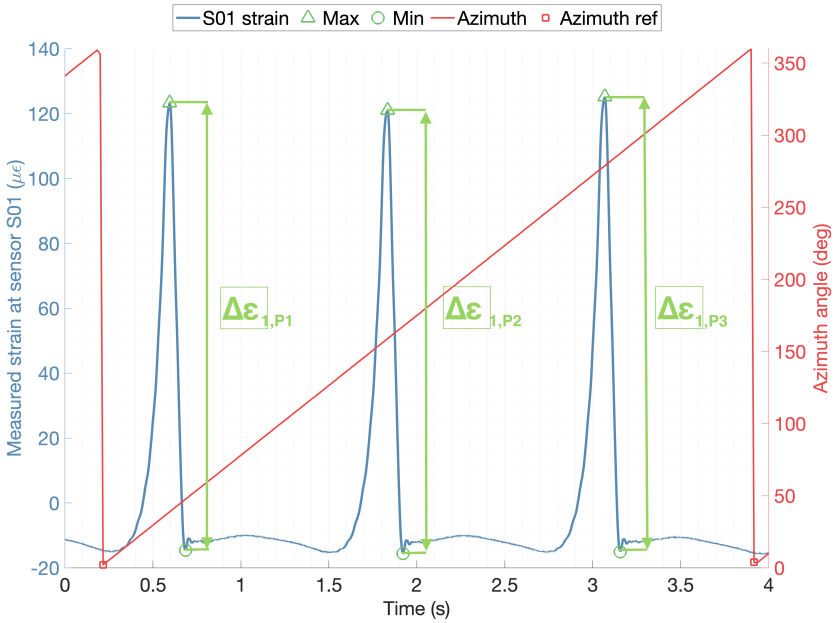

Figure 4. Peak-to-peak strain from sensor S01 assigned to P1, P2, and P3 for one full rotation.

is proposed to compare the strain of the simultaneous sensors. The peak-to-peak values are, therefore, weighted with the ratio between the average of all sensors and the mean peak-to-peak from each sensor. Figure 5 shows the first simultaneous mesh event recorded at sensors S01, S09, and S17 after the azimuth angle passed zero degrees. In this case, P1 meshes close to sensor S01, P2 is close to S17, and P3 is close to S09. Once the weighted peak-to-peak values have been assigned to the planet that caused the deformation, it is possible to compute an instantaneous K_γ for the time when the mesh was recorded. Figure 6 shows the torque and instantaneous K_γ value, constructed by repeating the same procedure for all eight sensor combinations with 24 values per rotor revolution, over an example 1 minute of turbine operation at 23:40 UTC on May 30. The torque ranges from 50% to near rated. The instantaneous load-sharing ranges from 0.97 to 1.03, but the average load-sharing for each planet is much closer to 1.0.

4. Field validation campaign

An extensive measurement campaign was conducted on the G97 2-MW wind turbine shown in Figure 1. The measurement and data acquisition equipment described in Section 2 were active from April 25 to July 31, 2023. During this period, the turbine was run under normal working conditions using the standard controller parameters. Data were continuously logged during operation using the specified sampling frequencies of each data source. The acquired data were binned into 10-minute files for ease of handling and analysis. Figure 7 shows a scatterplot constructed using the average wind speed against the total produced power for all the 10-minute recordings gathered during the test campaign. A wide range of operating conditions were covered and were considered representative of the complete power curve of the turbine. Only data containing produced power measurements above 150 kW were analyzed to evaluate the instantaneous mesh load factor. In total, 1644 10-minute files were recorded with a minimum of 150 kW, and 238 of these files had torque values above 50% of rated. As shown in Figure 6, the mesh load factor exhibits small fluctuations around a mean value. The effect of different

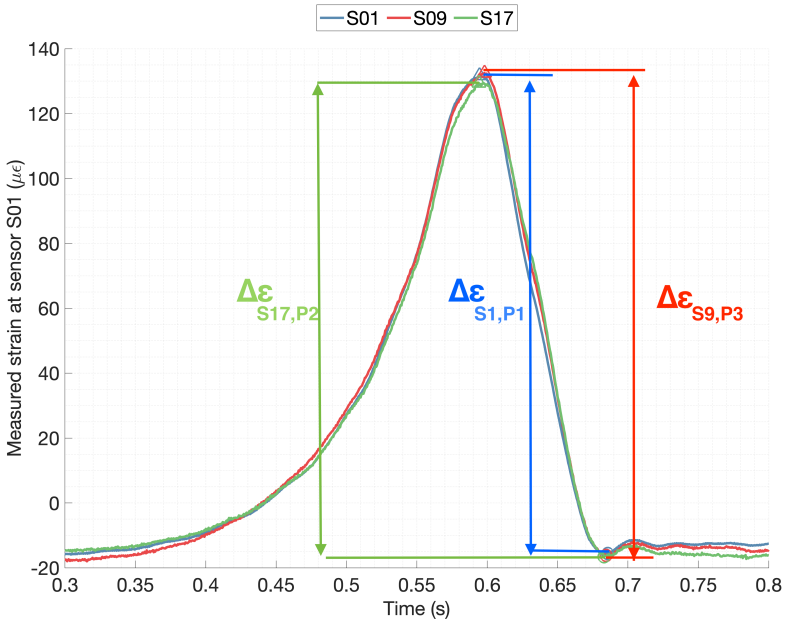

Figure 5. Strain of sensors S01, S09, and S17, zoom first peak, assignment of planets.

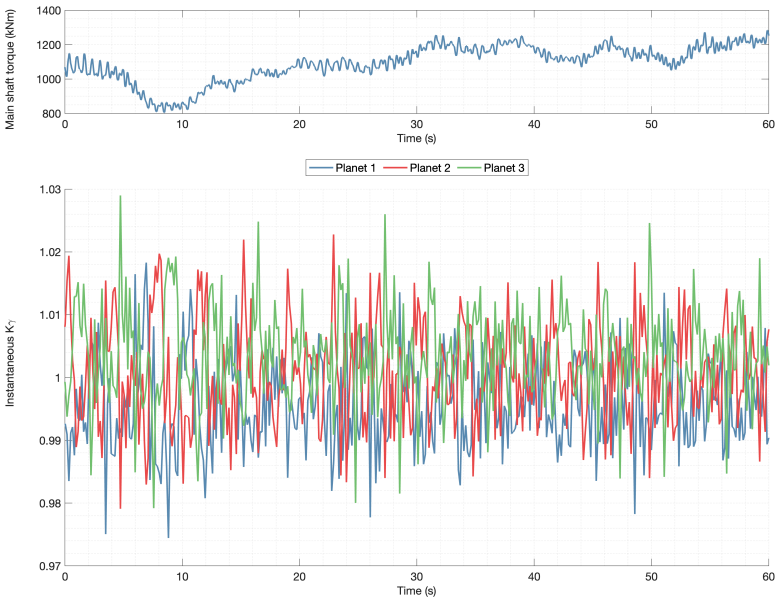

Figure 6. Evolution of torque and the mesh load factor with time (May 30 at 23:40 UTC).

normal power production operating conditions on the planet load-sharing behavior was analyzed by averaging the instantaneous K_γ values within the 10-minute recordings. From all the turbine operation parameters, torque was found to have the largest effect on the mesh load factor. Other turbine variables investigated included wind speed, wind turbulence intensity, wind direction,

yaw misalignment, blade pitch angles, and temperatures such as ambient, nacelle, ring gear and gearbox oil sump. The relationship between torque and mesh load factor is shown in Figure 8, where each dot represents the average value for a full revolution. As can be observed, all recorded values are very low, lower than 1.05 around the rated operation, and increase slightly for lower torques. This is expected because the effect of small manufacturing errors tends to be absorbed by the carrier's flexibility for higher torques. Furthermore, having a higher mesh load factor for such low torques is not critical for gear stresses. The effect of other operating variables like wind turbulence intensity and yaw misalignment was also investigated and found to be very low. These findings align with the gearbox's expected performance due to the drivetrain configuration and number of planets. The G97 wind turbine uses a four-point mount drivetrain, in which the overwhelming majority of nontorque loads are supported by the two main bearings, and the gearbox planetary stage comprises three planets and a floating sun, which minimizes the effect of any manufacturing errors. In Figure 8 the mean mesh load factor behavior is shown and found to align with each planet's intrinsic manufacturing properties. As shown in Figure 6, the mesh load factor exhibits a dynamic behavior. To quantify the deviation from the mean, Figure 9 shows the maximum mesh load factors recorded during full revolutions of the rotor. The difference between the maximum and average values are low for the planet with the highest mesh load factor, which validates the design assumptions used for gear rating and fatigue life calculations.

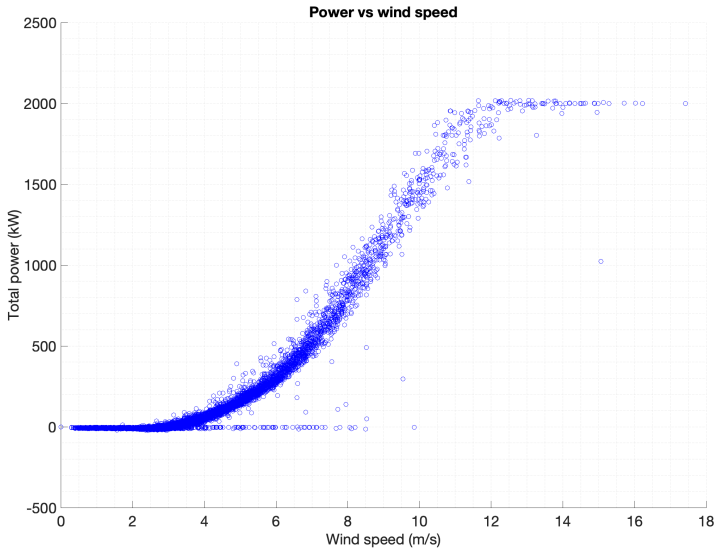

Figure 7. 10-minute average wind speed vs. total power produced by the turbine.

5. Conclusions

We have presented the results of an extensive field measurement campaign conducted on a 2-MW wind turbine gearbox. The results show that with an improved spacing definition, fiber-optic strain sensors placed on the outer surface of the static ring gear can provide a means to instantaneously evaluate the planetary mesh load factor. Accurate knowledge of planet load sharing is paramount to increasing torque density in new gearbox designs while ensuring high reliability. The instantaneous mesh load factor has been evaluated for a wide range of operating conditions over more than three months of normal operation, covering the complete power curve of the turbine. For operating conditions close to rated, the maximum mesh load factor was found to

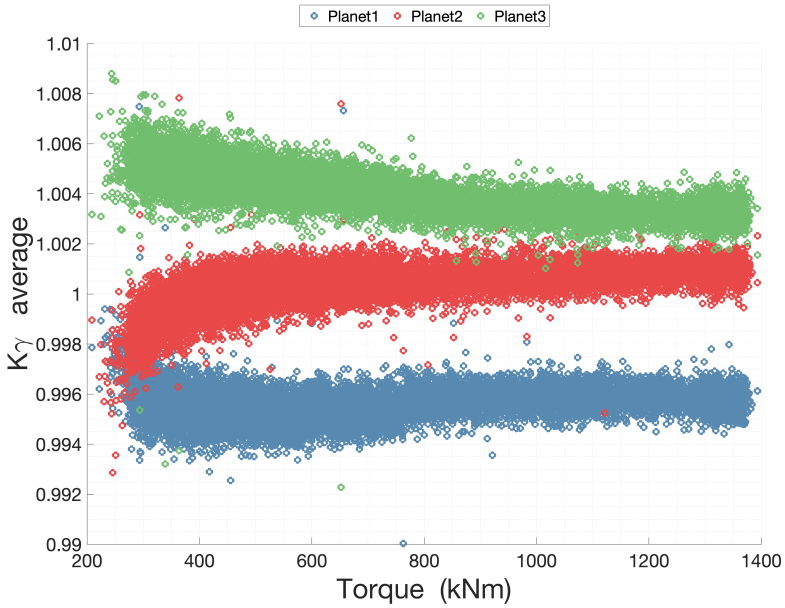

Figure 8. Average mesh load factor recorded during a full rotor revolution against rotor torque.

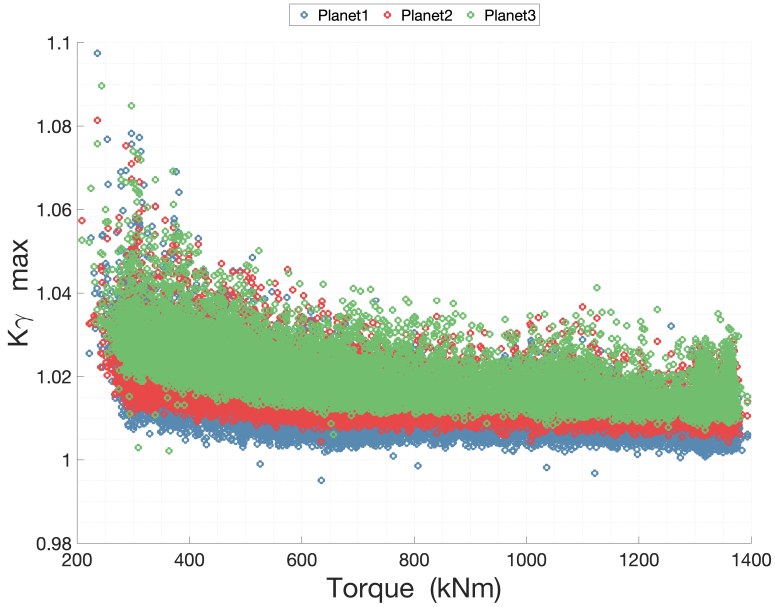

Figure 9. Maximum mesh load factor recorded during a full rotor revolution against rotor torque.

be below 1.05. This value is below the requirement of 1.10 from the IEC 61400–4 for three planets when no experimental data are available, which enables increasing the torque density of the gearbox. An increase in the mesh load factor was observed for lower torques, which is also to be expected but is not critical because tooth root and contact stresses are lower when torque decreases. The effects of other operating variables like wind turbulence intensity and

yaw misalignment on the mesh load factor were found to be negligible, which is aligned with the expected behavior of the four-point mount drivetrain configuration under test. For future work, it is suggested that an analytical model of planet load sharing could be developed and correlated with the measurements presented in this paper. Additionally, the potential usage of the presented instantaneous load mesh factor measurements for gearbox condition monitoring should be investigated.

`Acknowledgements` The authors wish to acknowledge financial support from Siemens Gamesa Renewable Energy and Sensing360 that made it possible to conduct the present study. This work was also authored in part by the National Renewable Energy Laboratory operated by the Alliance for Sustainable Energy, LLC, for the U.S. Department of Energy (DOE) under contract no. DE-AC36-08GO28308. Funding was provided by the U.S. Department of Energy Office of Energy Efficiency and Renewable Energy Wind Energy Technologies Office. The views expressed in the article do not necessarily represent the views of the DOE or the U.S. Government. The U.S. Government retains and the publisher, by accepting the article for publication, acknowledges that the U.S. Government retains a nonexclusive, paid-up, irrevocable, worldwide license to publish or reproduce the published form of this work, or allow others to do so, for U.S. Government purposes. The authors would also like to thank our NREL colleagues Jerry Hur, Brian Manoa, and Anna McAuliffe for their support during the sensor installation, and Jason Roadman and Scott Dana during the data acquisition process.

References

[1] P. Veers, K. Dykes, E. Lantz, S. Barth, C. L. Bottasso, O. Carlson, A. Clifton, J. Green, P. Green, H. Holttinen, D. Laird, V. Lehtomäki, J. K. Lundquist, J. Manwell, M. Marquis, C. Meneveau, P. Moriarty, X. Munduate, M. Muskulus, J. Naughton, L. Pao, J. Paquette, J. Peinke, A. Robertson, J. S. Rodrigo, A. M. Sempreviva, J. C. Smith, A. Tuohy, and R. Wiser, "Grand challenges in the science of wind energy," *Science*, vol. 366, no. 6464, p. eaau2027, 2019.

[2] ZF Wind Power, "ZF Wind Power breaks 200 Nm/kg torque density barrier with the modular gearbox platform SHIFT 7k." https://press.zf.com/press/en/releases/release_22016.html, 2020. Last accessed: 23 May 2023.

[3] Winergy, "High density gear units winergy-website." https://www.winergy-group.com/en/Products/Gear-Units/High-Density/p/HighDensityX, 2020. Last accessed: 23 May 2023.

[4] Gearbox by Gamesa. https://www.gamesagearbox.com/wind-technology/, 2023. Last accessed: 23 Jan 2024.

[5] U. Gutierrez Santiago, A. Fernández Sisón, H. Polinder, and J.-W. van Wingerden, "Input torque measurements for wind turbine gearboxes using fiber optical strain sensors," *Wind Energy Science*, vol. 7, no. 2, pp. 505–521, 2022.

[6] Y. Guo and J. Keller, "Validation of a generalized formulation for load-sharing behavior in epicyclic gears for wind turbines: Preprint," Tech. Rep. NREL/CP-5000-76380, National Renewable Energy Laboratory, 2020.

[7] I. 6336-1:2019, "Calculation of load capacity of spur and helical gears — Part 1: Basic principles, introduction and general influence factors," 2019.

[8] I. 61400-4:2012, "Wind turbines — Part 4: Design requirements for wind turbine gearboxes," 2012.

[9] U. Gutierrez Santiago, A. Fernández Sisón, H. Polinder, and J.-W. van Wingerden, "Experimental evaluation of the mesh load factor (K_γ) of a 6MW wind turbine gearbox," *J. Phys.: Conf. Ser.*, vol. 2265, no. 032003, 2022.

[10] A. Fernández Sisón, J. Calvo Irisarri, P. Olade Arce, and U. Gutierrez Santiago, "Load intensity distribution factor evaluation from strain gauges at the gear root," *Gear Solutions*, pp. 42–51, 2021.

[11] W. Meeusen, W. Ceulemans, and M. Otto, "Load distribution measurement on planetary gear systems," in *International Conference on Gears* (VDI, ed.), October 2010.